Altitude Optimization Based on TF Mini Plus LiDAR as a Guided System for Autonomous Drones in Inventory Management

M. Zotie Farkhani[1], Faiz Albar Risi[2], Ajie Rizki Kanedi[3], Fatahillah Hidayat[4], Fitriyanti Nakul[5]
Department of Electrical Engineering, Politeknik Negeri Batam, Batam, Kepulauan Riau, Indonesia

Article Info

Article history:

Received month dd, yyyy
Revised month dd, yyyy
Accepted month dd, yyyy

Keywords:

Drone
LiDAR
Autonomous
Inventory Management
Altitude Control
ROS

ABSTRACT

This research is an in-depth look at optimizing drone operations by integrating LiDAR sensors for more advanced altitude control, with a particular focus on inventory management. This study evaluates the performance of drones using three main sensors: Benewake TFmini Plus LiDAR, IMU Intel Realsense Tracking Camera, and Pixhawk Barometer. Autonomous drone missions included 5-meter and 10-meter forward flights, as well as obstacle recognition scenarios. Measurement datasets from 50 cm to 500 cm at 50 cm intervals were used as the basis for comparison of sensor accuracy and consistency. The experimental results illustrate the drone's dynamic response to LiDAR under various flight conditions, highlighting its adaptability and precision. This research makes a significant contribution to the understanding of the effectiveness of LiDAR sensors in height measurement, particularly in the context of inventory management in complex indoor environments. The findings stimulate further discussion on the potential development of autonomous drone technology for inventory management in the future.

Corresponding Author:

Fitriyanti Nakul, S.Pd., M.Si.

Department of Electrical Engineering, Politeknik Negeri Batam

Jl. Ahmad Yani, Kel. Teluk Tering, Kec. Batam Kota, Kota Batam, Kepulauan Riau 29461, Indonesia

Email: fitriyantinakul@polibatam.ac.id

1. INTRODUCTION

An Unmanned Aerial Vehicle (UAV), colloquially referred to as a drone, is an aircraft devoid of a human pilot that may be maneuvered remotely through the utilization of a remote control device[1],[2]. A range of frequently employed drone kinds can be identified, including Quadcopter, Fixed Wing, Military Drones, and others[3],[4].Drones possess a wide range of uses, one of which includes their deployment within various businesses[5],[6].An example of an application can be found within the industrial sector, specifically in the realm of warehouse inventory management.[7].

The utilization of drone systems in warehouse inventory management enables organizations to effectively monitor and control inventory, mitigate the risk of stock shortages or surpluses, and enhance operational efficiency. Through the use of this technology, the organization effectively maximizes the utilization of warehouse space[7],[8]. Furthermore, drone systems have the capability to facilitate precise and efficient inventory counts, hence mitigating potential human errors that may arise[9].

One example application of drone systems in warehouse inventory management is the utilization of these systems for the purpose of scanning barcode pictures[7] and RFID tags[9],[10].This particular function serves the purpose of identifying and categorizing various commodities inside the warehouse environment[7],[10].

In order to enhance operational efficiency in drone, it is imperative to consider a number of significant elements. Firstly, it is imperative to evaluate the issues of scanning speed and precision[11]. Additionally, the longevity of battery performance is a vital aspect in ensuring the seamless functionality of unmanned aerial vehicles[12]. In addition, it is imperative to take into account the significance of proficient navigation skills in order to guarantee optimal operational efficacy and efficiency of drones[13]. By taking into account these variables, Drone can function with optimal effectiveness and achieve a high degree of precision in the computation of inventory levels within storage facilities.

This research aims to examine the optimization of height in drone operations through the utilization of LiDAR sensors as navigational instruments[14][15]. LiDAR sensors possess the capability to furnish precise data pertaining to the altitude of the drone, hence facilitating the establishment of ideal altitude configurations to circumvent barriers and enhance the safety of

flying operations. Furthermore, the utilization of LiDAR sensors can facilitate the detection of objects in the vicinity of the unmanned aerial vehicle (UAV)[16].

2. METHOD

2.1 System Design

Figure 1 illustrates the comprehensive system overview. The various components of a system are divided into distinct functional units, each of which is responsible for carrying out separate actions that are relevant to the overall functioning of the system.

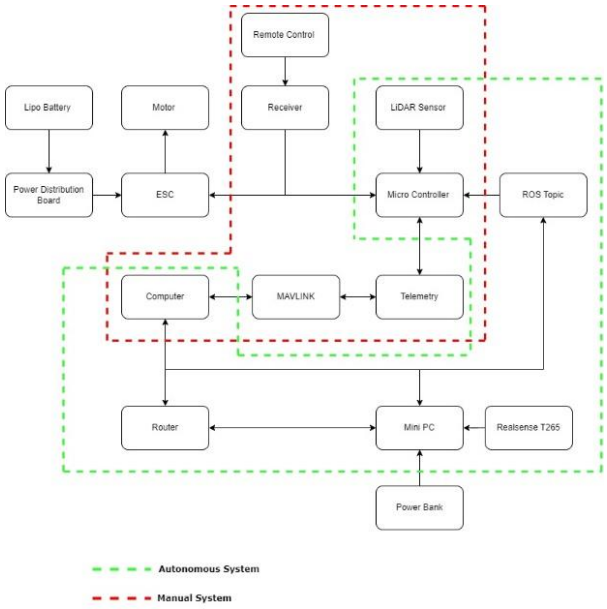

Figure 1. System design block diagram

The drone's technology can be operated through two distinct modes: manual and automatic. The manual approach entails the operator exerting direct control over the drone through a remote control device, whilst the automatic approach relies on the utilisation of algorithms and sensors to enable autonomous control of the drone's movement. The utilisation of an automated approach exhibits enhanced efficiency and a greater capacity to achieve heightened precision when executing tasks within an interior warehouse setting.

The use of drones for warehouse inventory management entails the utilization of a fully autonomous system. In the domain of autonomous flight, the transfer of control will occur to a mini PC that is linked to the flight controller. The communication protocol chosen for this project is Robot Operating System (ROS). The Raspberry Pi will operate as a server within the Ubuntu operating system.

2.2 Time-of-Flight (TOF)

The utilization of lidar technology in autonomous vehicles predominantly relies on the principle of Time-of-Flight (TOF). The term "TOF" refers to Time-of-Flight, which is a measurement technique used when a pulsed laser fires pulses either individually or continuously at a target. The internal timing circuit is instantaneously triggered upon the emission of a laser pulse. The calculator is utilized to determine the duration, denoted as Δt, between the arrival of the laser pulse at the target and its subsequent return to the receiver. This enables the calculation of the distance to the target[17],The schematic for time-of-flight (TOF) ranging is presented in Figure 2:

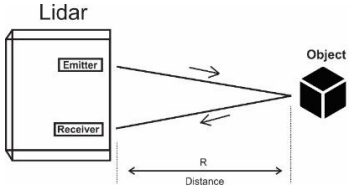

Figure 2. Shcematics of ToF

Δt is the temporal interval between the emission of a light pulse and its return to the receiver after being reflected by the target. This interval can be determined by multiplying the number of clock pulses, denoted as n, by the pulse interval τ[17].

$$R = \frac{1}{2} c n \tau = \frac{c}{2f} n = ln \quad (1)$$

The clock pulse frequency, denoted as f is the value for which it is being determined, $l = \frac{c}{2f}$, l each clock pulse indicates the distance base; n is by computing the number of clock pulses, the distance R of the target can be determined[17]. The symbol 'c' in the formula represents the constant speed of light, which is approximately 3 x 10^8 meters per second (m/s) in a vacuum.

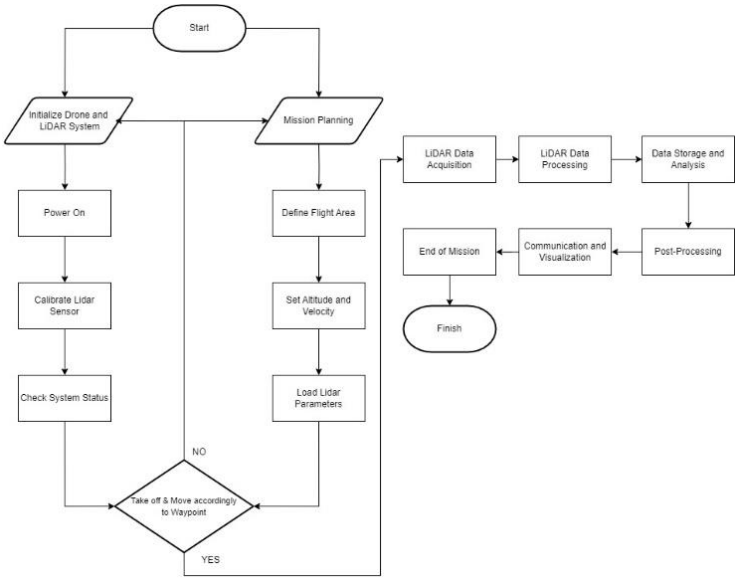

Figure 3. LiDAR Flowchart System

"Initialize Drone and LiDAR System" in the flowchart refers to the initial set of steps performed before the drone is launched and the LiDAR system is activated. In this stage, the drone is powered on and the LiDAR system is activated and calibrated to ensure that the LiDAR sensor is operating accurately. Then the overall system is checked to ensure that there are no problems or errors that could affect the operation of the drone and LiDAR. This includes verification of the battery, connectivity and other system functions.

"Mission Planning" is an important stage in the flowchart that involves determining the parameters and details of the mission before the drone is launched. At this stage, the user determines the area to be explored by the drone and determines the speed and altitude parameters of the drone using LiDAR according to the desired parameters for the purpose of the drone flight.

Figure 3 covers the crucial steps in using LiDAR technology on drones. The initial stage, "LiDAR Data Acquisition," describes the process of collecting data by activating the LiDAR sensor, initiating a scan while the drone is flying over the target area, and collecting 3D data points[18],[19]. Next, in the stage "LiDAR Data Processing," the data collected through scanning is processed. These steps include data preprocessing to remove noise, data transformation into point cloud form, and georeferencing to associate the data with a geographic coordinate system[20].

After data processing, the next step is "Data Storage and Analysis." At this stage, the processed data is stored and can be analyzed in real-time. This opens up opportunities for live monitoring and quick analysis during or after a drone mission[21],[22].

The "Post-Processing" process involves the creation of 3D models, generation of elevation maps, and feature extraction from the processed LiDAR data. This stage provides further information and allows for more specific applications, such as object identification or detailed mapping[23],[24].

"Communication and Visualization" are recognized in the next step, enabling data transmission to ground stations, real-time monitoring of data, and visualization of data for better understanding[22],[25]. The final step is to safely end the mission, i.e. "End of Mission," which involves returning the drone to the starting point, landing, and shutting down the system.

2.3 Robot Operating System (ROS)

The Robot Operating System (ROS), specifically ROS1 as the default version, is a framework that serves as a meta-operating system for the purpose of designing robotic systems (see to Figure 3). The Robot Operating System (ROS) facilitates the operation of autonomous computer processes known as nodes, which are supported by a master node, parameter server, and middleware layer. These systems enable the exchange of information between nodes through the utilization of topics and services[26].

The primary utility of the Robot Operating System (ROS) The roscore component encompasses the ROS master, parameter server, and the rosout node. The master node is responsible for monitoring and managing the available topics and services, as well as maintaining a comprehensive map of the geographical distribution of all nodes. Regrettably, the master node lacks the capability to enforce this mapping, hence giving rise to numerous vulnerabilities [27][28] within the ROS system.The parameter server serves as a centralized storage system for the nodes, allowing them to access and share global variables. The master node utilizes XMLRPC function calls for communication, which introduces many vulnerabilities[26].

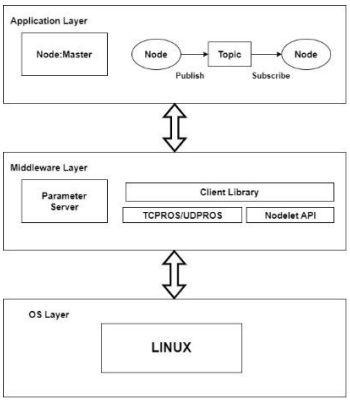

Figure 4. The Architecture of ROS1

3. RESULTS AND DISCUSSION

The chapter results and discussion presents an in-depth analysis of the data generated during the drone flight. The focus shifts to the comparison of the Z pose data between the actual output and the sensor used, which includes an evaluation of the accuracy and consistency in reproducing the vertical position of the object during the mission. Furthermore, the study explored the 3D visualization of the trajectory on the Z axis using matplotlib, providing a clear picture of the response of the Lidar sensor to changes in the drone's position. These two aspects underlie the assessment of the sensor's reliability and performance in the face of flight dynamics. A detailed analysis of the Z pose data and 3D trajectory visualization is a critical cornerstone in understanding the level of sensor precision and its implications on the success of data collection during drone flight missions.

3.1. Z Pose Data Comparison

In the context of this research, a dataset consisting of ten consecutive values has been obtained, starting from 50 cm in the first sequence until it reaches 500 cm in the tenth sequence. Each value in this dataset has a fixed interval of 50 cm, which indicates the incremental value of each successive measurement step. It is important to note that the actual data is measured in centimeters of length. The existence of actual data is crucial in this research methodology, where it will serve as the basis of comparison for the information generated by the three sensors used on the drone, namely the Benewake TFmini Plus LiDAR, IMU Intel Realsense Tracking Camera, and Barometer Pixhawk.

The three sensors function as altitude measuring devices on the drone. This research design aims to assess and compare the accuracy and consistency of the measurement results of the three sensors. In-depth analysis of this dataset is expected to significantly contribute to the understanding of the performance of these sensors in the context of altitude measurement in drone flight environments.

Table 1. Z Axis Comparison

Z Axis Comparison (cm)				
No.	Actual	Benewake TFmini Plus LiDAR	IMU Intel Realsense Tracking Camera	Barometer Pixhawk
1	50	50	59	103
2	100	102	109	176
3	150	147	158	221
4	200	197	207	244
5	250	246	264	295
6	300	297	319	327
7	350	350	379	360
8	400	398	436	392
9	450	446	494	465
10	500	497	550	510

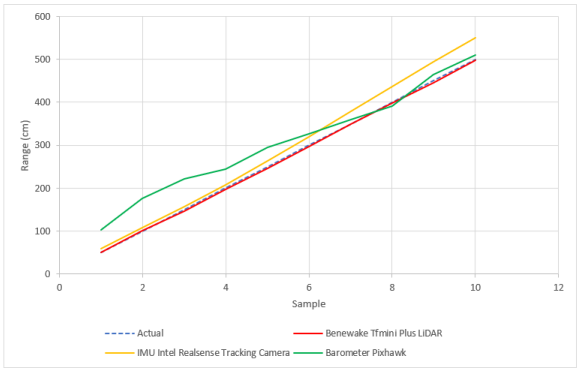

Figure 5. Comparison Chart

Utilizing the Mean Absolute Error (MAE) for the computation of the accuracy error between the sensor's output and the true position.

$$MAE = \frac{1}{n}\sum_{i=1}^{n} |Approximation_i - Actual_i| \quad (2)$$

$$\%Error = \left(\frac{MAE}{Mean\ of\ Actual\ Values}\right) \times 100 \quad (3)$$

Table 2. Error Rate on Z axis

Error Rate on Z axis		
Benewake TFmini Plus LiDAR	IMU Intel Realsense Tracking Camera T265	Barometer Pixhawk
0.945%	9.527%	17.527%

3.2. Z Axis Visual 3D Trajectory

In this study, the drone was run autonomously with a speed of 0.2 m/s and a height of 0.9 meters while capturing 3D trajectory data on the Z-axis. The experiments involved 5-meter and 10-meter forward flight missions, as well as an obstacle recognition scenario in the middle of the path. Each mission begins with a take-off process and ends with a landing procedure, forming a series of coordinated autonomous flight tasks.

The drone's involvement in the action gives a dynamic dimension to the data capture, creating a context that not only goes in-depth in detailing the response of the Lidar sensor to changes in the drone's position, but also reveals the drone's ability to navigate automatically through a wide variety of missions.

3.2.1. Forward 5 meters

In this first subsection, the drone performed a 5-meter forward mission with a speed of 0.2 m/s and a height of 0.9 meters. The 3D trajectory data capture on the Z-axis is done by involving the three sensors mentioned earlier: Lidar, IMU Realsense Tracking Camera, and Barometer. The presence of these three sensors makes the dataset more comprehensive, enabling a holistic understanding of the Lidar sensor's response to changes in drone position during flight. This exploration forms the basis for assessing the drone's performance in achieving the 5-meter autonomous flight target.

Red = Benewake TFmini Plus LiDAR
Blue = IMU Intel Realsense Tracking Camera T265
Green = Barometer Pixhawk

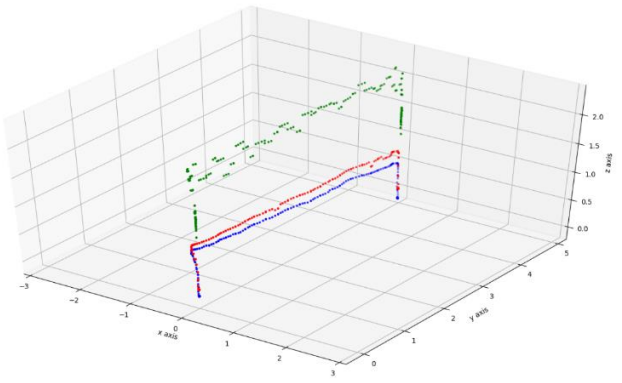

Start Range
```
lidar = 0.11999998986721039
baro = 1.316
realsense = -0.003294056048616767
```

Fly Range
```
lidar = 0.9120000004768372
baro = 2.212
realsense = 0.7369077205657959
```

Finish Range
```
lidar = 0.12999999523162842
baro = 1.234
realsense = -0.03747941181063652
```

Figure 6. 3D Visual Trajectory: Drone Autonomous Forward Flight Mission 5 Meter (Isometric View)

3.2.2. Forward 10 meters

In the second subsection, the drone performed a 10-meter forward mission with a speed of 0.2 m/s and a height of 0.9 meters. The process of capturing 3D trajectory data on the Z-axis also involves the three sensors mentioned earlier: Lidar, IMU Realsense Tracking Camera, and Barometer. The participation of these three sensors contributes to a more complete dataset, strengthening the understanding of the Lidar sensor's response to changes in drone position during flight. As such, this exploration provides a critical basis for evaluating the drone's ability to achieve the 10-meter autonomous flight target.

Red = Benewake TFmini Plus LiDAR
Blue = IMU Intel Realsense Tracking Camera T265
Green = Barometer Pixhawk

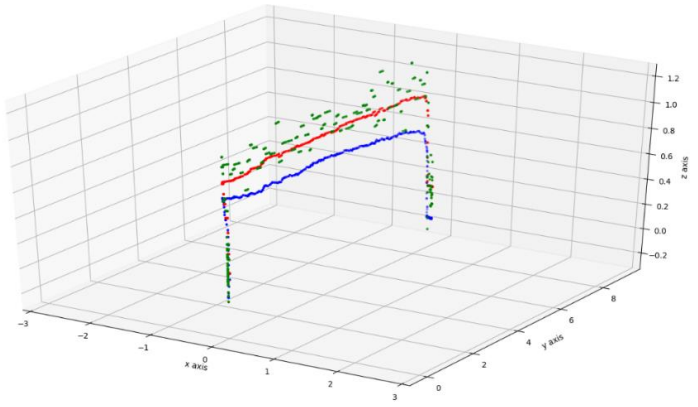

Start Range
```
lidar = 0.12999999523162842
baro = 0.127
realsense = -0.13366644084453583
```
Fly Range
```
lidar = 0.9120000004768372
baro = 1.031
realsense = 0.663575291633606
```
Finish Range
```
lidar = 0.12999999523162842
baro = -0.011
realsense = -0.13281551003456116
```

Figure 7. 3D Visual Trajectory: Drone Autonomous Forward Flight Mission 10 Meter (Isometric View)

3.2.3. Object Detection Analysis: LiDAR on Drones Overcomes Obstacles

This third subsection focuses on the analysis of LiDAR data on a drone that generates a 3D trajectory during a 3-meter flight with a height of 1 meter. On the flight path, a box-shaped object with a height of 12 cm was placed in the center. It is important to note that the LiDAR configuration is set such that the sensor does not identify the box as an obstacle since the height of the object does not exceed 20 cm.

The adjustment aims to keep the drone maintaining its true altitude at 1 meter off the ground from the beginning to the end of the flight mission. This process involves processing data obtained from ROS topics, especially the rangefinder, which is then processed using the Python programming language. The results of this 3D trajectory analysis are expected to provide in-depth insights into the LiDAR response to obstructing objects and its implications for drone travel during flight missions.

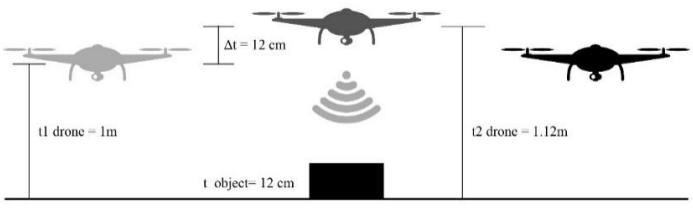

Figure 8. LiDAR Altitude Control: Drone Response to Obstacle Detection

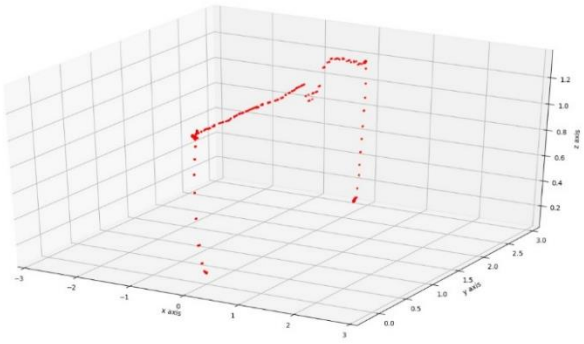

Figure 9. 3D Trajectory Visualization: LiDAR Data During Flight Testing (Isometric View)

In Figure 8, there is an illustration of a drone equipped with a LiDAR sensor flying at an altitude of 1 meter. As the drone approaches a 12 cm obstacle, LiDAR detects it and the drone quickly adjusts its altitude to avoid the obstacle. This illustration shows the dynamic response of LiDAR in ensuring the drone maintains a precise altitude, emphasizing the effective use of this technology in drone navigation.

Figure 9 shows the 3D trajectory of the drone during the test flight with the LiDAR sensor. This visualization, created using matplotlib, reflects the LiDAR's real-time response to changes in altitude and ambient terrain. It provides a brief but comprehensive overview of the LiDAR's performance in mapping and monitoring the drone's altitude during flight.

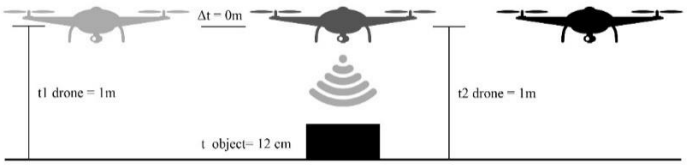

Figure 10. Adaptive LiDAR Sensing for Low Obstacle Avoidance

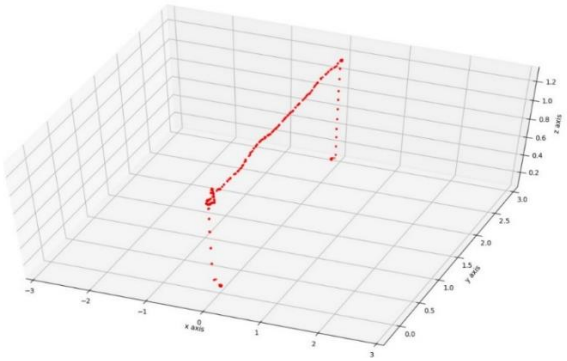

Figure 11. Integrated 3D Trajectory Following Adaptive LiDAR Settings (Isometric View)

Figure 10 shows an illustration of a drone with a LiDAR sensor that can process data from ROS topics to recognize objects below 20 cm in height as non-obstacles. With smart settings, the LiDAR ensures that the drone stays at a height of 1 meter when passing over such objects. This illustration reflects LiDAR's ability to be adaptive to specific situations, effectively enhancing the drone's height control.

Figure 11 shows the 3D trajectory of the drone during flight, continuing from the illustration in Figure 10 where LiDAR recognizes objects below 20 cm in height as non-obstacles. This visualization, created through matplotlib, provides a complete picture of the LiDAR response to environmental changes. This graph shows how the drone, thanks to the LiDAR's adaptability to ROS data, manages to maintain its flight path without perceiving the object as an obstacle. Figure 11 provides further insight into the LiDAR's ability to respond to dynamic changes during drone flight.

4. CONCLUSION

This study offers a thorough examination of the drone's performance and the three sensors employed. It presents valuable insights by comparing Z posture data, visualizing the 3D trajectory in the Z axis, and analyzing LiDAR data collected during autonomous flight. The Z pose data serves as a significant criterion for mission success by assessing the precision and consistency of the sensors in replicating the vertical position of objects. The utilization of LiDAR, IMU Intel Realsense Tracking Camera, and Barometer in a 3D trajectory visualization aids in comprehending the LiDAR's reaction to alterations in the drone's position. By utilizing real datasets with a 50 cm interval, a comprehensive evaluation of the three sensors was conducted,

highlighting the exceptional performance of LiDAR as a highly efficient height sensor, particularly in indoor settings. The autonomous drone studies showcased the drone's versatility in many missions, such as 5-meter and 10-meter missions, as well as obstacle identification scenarios. The successful avoidance of a 12 cm high obstacle by a drone during a 3-meter flight, as demonstrated by LiDAR analysis, underscores the dependability of LiDAR as a height sensor, particularly in intricate indoor settings. Consequently, it is highly recommended to utilize LiDAR as a height sensor on drones, particularly in light of the swift advancement of autonomous drone technology. The percentage errors (%Error) for LiDAR, Realsense IMU, and Baro Pixhawk are 0.945%, 9.527%, and 17.527%, respectively. These results demonstrate the superior performance of LiDAR and provide strong justification for recommending its use.

ACKNOWLEDGEMENTS

I would want to thank everyone who helped me to finish this study project. A special thank you to my adviser for all of her help and support throughout the years. I am grateful to Batam State Polytechnic for providing vital resources, particularly the BRAIL and its administrators. We appreciate the insightful comments from participants and contributors as well as the support and encouragement from colleagues. Finally, I would want to express my gratitude to my family and friends for their constant support during this academic journey.

REFERENCES

[1] R. Amin, L. Aijun, and S. Shamshirband, "A review of quadrotor UAV: control methodologies and performance evaluation," *Int. J. Autom. Control*, vol. 10, no. 2, p. 87, 2016, doi: 10.1504/IJAAC.2016.076453.

[2] H. Shakhatreh *et al.*, "Unmanned Aerial Vehicles (UAVs): A Survey on Civil Applications and Key Research Challenges," *IEEE Access*, vol. 7, pp. 48572–48634, 2019, doi: 10.1109/ACCESS.2019.2909530.

[3] O. Tatale, N. Anekar, S. Phatak, and S. Sarkale, "Quadcopter: Design, Construction and Testing," *Int. J. Res. Eng. Appl. Manag.*, vol. 4, no. AMET-2018, pp. 1–7, 2018.

[4] O. I. D. Bashi, W. Z. W. Hasan, N. Azis, S. Shafie, and H. Wagatsuma, "Unmanned Aerial Vehicle Quadcopter: A Review," *J. Comput. Theor. Nanosci.*, vol. 14, no. 12, pp. 5663–5675, Dec. 2017, doi: 10.1166/jctn.2017.7049.

[5] K. Nonami, "Drone Technology, Cutting-Edge Drone Business, and Future Prospects," *J. Robot. Mechatronics*, vol. 28, no. 3, pp. 262–272, Jun. 2016, doi: 10.20965/jrm.2016.p0262.

[6] B. Sah, R. Gupta, and D. Bani-Hani, "Analysis of barriers to implement drone logistics," *Int. J. Logist. Res. Appl.*, vol. 24, no. 6, pp. 531–550, Nov. 2021, doi: 10.1080/13675567.2020.1782862.

[7] H. Cho, D. Kim, J. Park, K. Roh, and W. Hwang, "2D Barcode Detection using Images for Drone-assisted Inventory Management," in *2018 15th International Conference on Ubiquitous Robots (UR)*, IEEE, Jun. 2018, pp. 461–465. doi: 10.1109/URAI.2018.8441834.

[8] Y. Shen, X. Xu, B. Zou, and H. Wang, "Operating policies in multi-warehouse drone delivery systems," *Int. J. Prod. Res.*, vol. 59, no. 7, pp. 2140–2156, Apr. 2021, doi: 10.1080/00207543.2020.1756509.

[9] J. Quino, J. M. Maja, J. Robbins, R. T. Fernandez, J. S. Owen, and M. Chappell, "RFID and Drones: The Next Generation of Plant Inventory," *AgriEngineering*, vol. 3, no. 2, pp. 168–181, Apr. 2021, doi: 10.3390/agriengineering3020011.

[10] B. Rahmadya, R. Sun, S. Takeda, K. Kagoshima, and M. Umehira, "A Framework to Determine Secure Distances for Either Drones or Robots Based Inventory Management Systems," *IEEE Access*, vol. 8, pp. 170153–170161, 2020, doi: 10.1109/ACCESS.2020.3024963.

[11] R. Kamnik, M. Nekrep Perc, and D. Topolšek, "Using the scanners and drone for comparison of point cloud accuracy at traffic accident analysis," *Accid. Anal. Prev.*, vol. 135, no. April 2019, p. 105391, Feb. 2020, doi: 10.1016/j.aap.2019.105391.

[12] J. Kim, Y. Choi, S. Jeon, J. Kang, and H. Cha, "Optrone: Maximizing Performance and Energy Resources of Drone Batteries," *IEEE Trans. Comput. Des. Integr. Circuits Syst.*, vol. 39, no. 11, pp. 3931–3943, Nov. 2020, doi: 10.1109/TCAD.2020.3012790.

[13] S. Jung, S. Hwang, H. Shin, and D. H. Shim, "Perception, Guidance, and Navigation for Indoor Autonomous Drone Racing Using Deep Learning," *IEEE Robot. Autom. Lett.*, vol. 3, no. 3, pp. 2539–2544, Jul. 2018, doi: 10.1109/LRA.2018.2808368.

[14] M. Bolognini and L. Fagiano, "LiDAR-Based Navigation of Tethered Drone Formations in an Unknown Environment," *IFAC-PapersOnLine*, vol. 53, no. 2, pp. 9426–9431, 2020, doi: 10.1016/j.ifacol.2020.12.2413.

[15] S. Suzuki, "Integrated Navigation for Autonomous Drone in GPS and GPS-Denied Environments," *J. Robot. Mechatronics*, vol. 30, no. 3, pp. 373–379, Jun. 2018, doi: 10.20965/jrm.2018.p0373.

[16] N. A. Fuad *et al.*, "Accuracy evaluation of digital terrain model based on different flying altitudes and conditional of terrain using UAV LiDAR technology," *IOP Conf. Ser. Earth Environ. Sci.*, vol. 169, no. 1, p. 012100, Jul. 2018, doi: 10.1088/1755-1315/169/1/012100.

[17] J. Liu, Q. Sun, Z. Fan, and Y. Jia, "TOF Lidar Development in Autonomous Vehicle," in *2018 IEEE 3rd Optoelectronics Global Conference (OGC)*, IEEE, Sep. 2018, pp. 185–190. doi: 10.1109/OGC.2018.8529992.

[18] K. Bakuła, A. Salach, D. Zelaya Wziątek, W. Ostrowski, K. Górski, and Z. Kurczyński, "Evaluation of the accuracy of lidar data acquired using a UAS for levee monitoring: preliminary results," *Int. J. Remote Sens.*, vol. 38, no. 8–10, pp. 2921–2937, May 2017, doi: 10.1080/01431161.2016.1277044.

[19] L. G. Pereira, P. Fernandez, S. Mourato, J. Matos, C. Mayer, and F. Marques, "Quality control of outsourced LiDAR

data acquired with a UAV: A case study," *Remote Sens.*, vol. 13, no. 3, pp. 1–12, 2021, doi: 10.3390/rs13030419.
[20] B. Lohani and S. Ghosh, "Airborne LiDAR Technology: A Review of Data Collection and Processing Systems," *Proc. Natl. Acad. Sci. India Sect. A Phys. Sci.*, vol. 87, no. 4, pp. 567–579, Dec. 2017, doi: 10.1007/s40010-017-0435-9.
[21] H. Chen, F. Gao, Q. Zhu, Q. Yan, D. Hua, and S. Stanič, "Storage method of multi-channel lidar data based on tree structure," *Sci. Rep.*, vol. 12, no. 1, p. 9075, May 2022, doi: 10.1038/s41598-022-13138-9.
[22] O. Kreylos, G. W. Bawden, and L. H. Kellogg, "Immersive Visualization and Analysis of LiDAR Data," in *Lecture Notes in Computer Science (including subseries Lecture Notes in Artificial Intelligence and Lecture Notes in Bioinformatics)*, vol. 5358 LNCS, no. PART 1, 2008, pp. 846–855. doi: 10.1007/978-3-540-89639-5_81.
[23] X. Huang, L. Zhang, and W. Gong, "Information fusion of aerial images and LIDAR data in urban areas: vector-stacking, re-classification and post-processing approaches," *Int. J. Remote Sens.*, vol. 32, no. 1, pp. 69–84, Jan. 2011, doi: 10.1080/01431160903439882.
[24] K. Liu, H. Ma, H. Ma, Z. Cai, and L. Zhang, "Building Extraction from Airborne LiDAR Data Based on Min-Cut and Improved Post-Processing," *Remote Sens.*, vol. 12, no. 17, p. 2849, Sep. 2020, doi: 10.3390/rs12172849.
[25] C. V. Poulton *et al.*, "Long-Range LiDAR and Free-Space Data Communication With High-Performance Optical Phased Arrays," *IEEE J. Sel. Top. Quantum Electron.*, vol. 25, no. 5, pp. 1–8, Sep. 2019, doi: 10.1109/JSTQE.2019.2908555.
[26] S. Rivera, A. K. Iannillo, S. Lagraa, C. Joly, and R. State, "ROS-FM: Fast Monitoring for the Robotic Operating System(ROS)," in *2020 25th International Conference on Engineering of Complex Computer Systems (ICECCS)*, IEEE, Oct. 2020, pp. 187–196. doi: 10.1109/ICECCS51672.2020.00029.
[27] A. Koubaa, "ROS As a Service: Web Services for Robot Operating System," *J. Softw. Eng. Robot.*, vol. 1, no. 1, pp. 123–126, 2015, [Online]. Available: https://www.researchgate.net/publication/309668701
[28] P. Estefo, J. Simmonds, R. Robbes, and J. Fabry, "The Robot Operating System: Package reuse and community dynamics," *J. Syst. Softw.*, vol. 151, pp. 226–242, May 2019, doi: 10.1016/j.jss.2019.02.024.